



# IMPLICATIONS OF A DOWN-STAND BEAM ON THE CEILING FLAME EXTENSION CHARACTERISTICS IN A LARGE-SCALE CLT ENCLOSURE FIRE EXPERIMENT

Danny Hopkin<sup>1</sup>, Michael Spearpoint<sup>1</sup>, Renaud Blondeau<sup>2</sup>, Tim Sleik<sup>3</sup>, Harald Krenn<sup>4</sup>, Gordian Stapf<sup>5</sup> & Wojciech Węgrzyński<sup>6</sup>

**ABSTRACT:** This paper provides further understanding of the fire performance of exposed cross-laminated timber (CLT) in large enclosures. An office-type configuration has been represented by a 3.75 by 7.6 by 2.4 m high enclosure constructed of non-combustible blockwork walls, with a large opening on one long face. Two experiments are described in which propane-fuelled burners created a line fire that impinged on CLT ceilings. The first experiment had a smooth CLT soffit, with the CLT formed from 160 mm thick panels (40-20-40-20-40 mm). The second experiment adopted the same CLT but included a 400 mm deep, 200 mm wide glulam beam half-way along the length of the enclosure. In both experiments, the lamella of each CLT were bonded using a standard polyurethane adhesive. The facing lamella of the CLT was not edge bonded. The results indicate the importance of consideration of the impact of ceiling protrusions, such as down-stand beams, with differences in both radiative heat flux to the ceiling and floor observed between the two cases. Considering large contemporary open plan office enclosures, this would likely translate to differences in spread rate within an enclosure and time to auto-extinction of flaming combustion which should be addressed by designers.

**KEYWORDS:** cross-laminated timber; auto-extinction; flame spread; glulam; ceiling protrusion

## 1 INTRODUCTION & MOTIVATION

When conceiving of a new office building in the UK, timber is increasingly considered as part of any potential framing solution. This is driven by a combination of embodied carbon, aesthetics, and constructability considerations. Commercial premises, such as offices, often have specific user/client demands, with emphasis placed on high floor-to-ceiling heights, long spans between column members and large areas of glazing. For this reason, the UK market is converging upon hybrid construction solutions where timber, in the form of cross-laminated-timber (CLT), is used in concert with other materials, such as steel and concrete.

Recent guidance has been published [1] which has clarified the design evidence that should be provided by engineers when demonstrating that an adequate level of structural fire performance will be achieved when adopting a combustible structural framing solution. In higher consequence of failure buildings, e.g., medium- to high-rise offices, the structure must be designed in a manner whereby it has a reasonable likelihood of surviving the full duration of a fire. This necessitates that if the structure becomes involved as a source of fuel, combustion must cease and the structure should remain capable of supporting the applied loads both during and

beyond a fire. The cessation of combustion is generally taken to be that of flaming, with some expectation that fire service intervention is necessary to stop any subsequent smouldering combustion.

To design a structure to undergo auto-extinction of flaming combustion, there needs to be an understanding of: (a) the fire dynamics in the enclosure, in particular spread rates; and (b) the heat flux to the combustible structural elements. Both are likely to be impacted by the presence of ceiling protrusions, such as beams. To date, limited effort has been committed to understanding the importance of such protrusions, other than at reduced scale [2].

This paper, as part of a larger experimental campaign by the Structural Timber Association (STA) special interest group on CLT enclosure fire dynamics, reports on two large-scale experiments that compare fire behaviour of engineered timber ceilings (comprising CLT and glulam) both with and without a beam protrusion.

## 2 THE EXPERIMENTS

### 2.1 The fire enclosure

The geometry of the fire enclosure was chosen to: (a) ensure CLT spans were broadly aligned to that commonly

<sup>1</sup> OFR Consultants, Sevendale House, Lever St, Manchester M1 1JA, UK, [danny.hopkin@ofrconsultants.com](mailto:danny.hopkin@ofrconsultants.com)

<sup>2</sup> Stora Enso Oyj, Wood Product - Building Solutions, PL 309, 00101 Helsinki, Finland

<sup>3</sup> Binder Holz GmbH, Zillertal Straße 39 · A, 6263 Fügen, Austria

<sup>4</sup> KLH Massivholz GmbH, Gewerbestraße 4, 8842 Teufenbach-Katsch, Austria

<sup>5</sup> Henkel & Cie. AG, Industriestrasse 17a, Sempach Station, 6203 Neuenkirch, Switzerland

<sup>6</sup> Instytut Techniki Budowlanej (ITB), Filtrowa 1, 00-611 Warszawa, Poland

adopted in hybrid commercial (office) construction, with the CLT spanning 3.75 m from front to back, and (b) to be as large as feasible within the constraints of the laboratory, considering both footprint and anticipated maximum heat release rate (HRR). This led to an enclosure of internal dimensions of 3.75 m (depth) by 7.6 m (width) by 2.4 m (height). The enclosure of the rig was constructed from exposed lightweight concrete blockwork that was 240 mm thick. Given commercial construction is typically characterised by a large amount of perimeter glazing, one elevation of the rig featured a large permanent opening, measuring 7.6 m wide and 2.0 m high. To allow for the characterisation of potential external flames from the opening, a mock-up façade extension was included. This extended the full width of the enclosure, measuring 2.6 m in height, with a down-stand that extended 0.4 m below the CLT soffit.

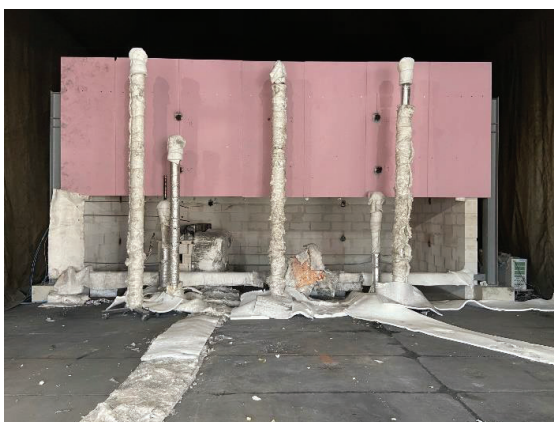


**Figure 1:** Image of the enclosure with the propane gas burners shown at the quarter point.

## 2.2 The mass timber elements

In all cases, the CLT was 160 mm thick, with lay-up 40-20-40-20-40 mm lamellae. At the time of the experiments, the estimated moisture content of the CLT slabs was in the range of 12–14% by mass. Non-edge-bonded CLT was chosen in both experiments with the intent of realising a lower bound of fire performance, i.e., the lack of edge-bonding can permit the rapid development of gaps between CLT facing lamella upon heating and subsequent dehydration, followed by pyrolysis. In both experiments, lamellae were bonded with a standard polyurethane (PUR) adhesive (Henkel Loctite HB S).

The first experiment had a smooth exposed CLT ceiling, i.e., no ceiling protrusions. This is henceforth referred to as the “no beam” case. The second “with beam” experiment included glulam beam measuring 200 mm wide by 400 mm deep. This was fixed to slab 3, such that the beam edge aligned with the joint to slab 2. The glulam beam was fixed to the slab from below, using stirrups. These comprised a universal bracket commonly used for propping ventilation ducts from below, which were supported on threaded tension rods on each side.

Slabs are distinguished in the discussion of instrumentation and loading, see Figure 4.

## 2.3 Fire source

The ceiling was heated using propane gas burners, elevated to sit 1 m below the soffit. The burner array comprised of 6 burners, each measuring 150 × 300 mm on plan, configured to achieve a rectangle measuring 300 × 900 mm. The burners were located off-centre (at the quarter point), with the aim of inducing flame extension to 50% of the ceiling length in a reference experiment reported elsewhere [3] and a heat flux exceeding 120 kW/m<sup>2</sup> at the plume centreline. The HRR of the fire was controlled via mass flow switches, leading to a HRR that ramped to a maximum of 1250 kW (achieved over an 8 min period in 250 kW steps). The duration of steady heating (at 1250 kW) for the exposed CLT experiments was chosen to induce significant char fall-off in the smooth soffit experiment (above the burner), resulting in a steady phase duration of 80 min. After this phase, the burners ramped down in 250 kW increments every 5 min, before being switched off, see Figure 2. An image of the burner impinging on the ceiling is given in Figure 3.

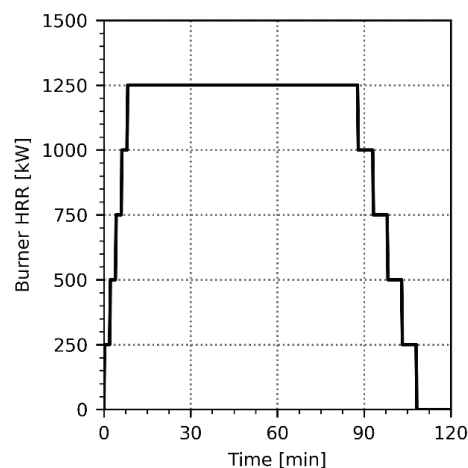


**Figure 2:** Burner heat release rate with time.



**Figure 3:** Image of burner and ceiling jet, “no beam” experiment 1.

## 2.4 Instrumentation and loading

The enclosures were instrumented using a combination of bead and plate thermocouples and water-cooled heat flux gauges. CLT slabs were loaded to achieve a nominally uniformly distributed load of 153 kg/m<sup>2</sup>, or c. 4300 kg in total. Slab displacement was monitored, and CLT mass loss rate (MLR) estimated from load-cells. The experiments were identical, other than the inclusion of a glulam beam in the second experiment. Key dimensions and locations of instrumentation are shown in Figure 4.

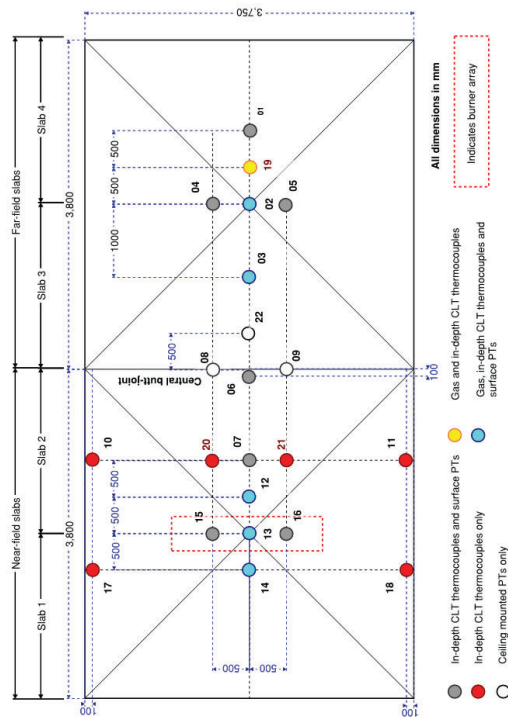


**Figure 4:** Enclosure plan showing key enclosure dimensions, measurement locations and references, slab locations and burner array position.

The CLT support structure comprised a perimeter steel frame, from which each pair of CLT slabs were suspended via tension rods. In line with these tension rods were a load cell to each corner, i.e., eight in total, recording the tensile load acting on the supports. The arrangement is as shown indicatively in Figure 5. The slabs sat within the perimeter of blockwork wall enclosure, ensuring the CLT and supporting structure were not propped by the perimeter wall. Minor gaps at the ceiling edges were fire stopped with mineral wool.

## 3 RESULTS

The emphasis of the results in this paper are on the fire development characteristics, i.e., no comment is made on the charring rates or mechanical performance associated with the engineered timber ceilings. To this end, results are presented in terms of the ceiling mass loss and heat

release rate (HRR), gas temperatures below the ceiling, estimated radiative heat flux to the ceiling and floor, and the heat flux opposing the opening. Each are discussed in the sub-sections that follow.

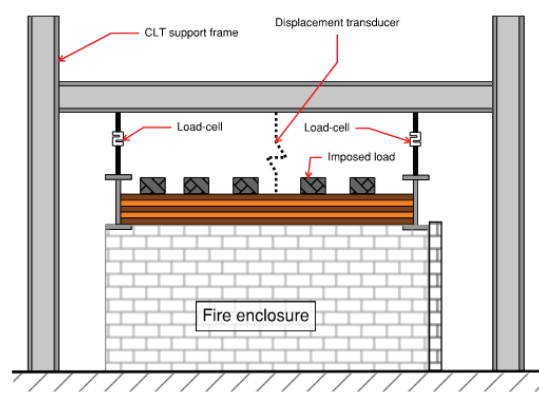


**Figure 5:** Illustrative section through the rig showing CLT support mechanism, including load cells and displacement transducers.

### 3.1 Timber mass loss and estimated HRR

The eight load-cells were summed and normalised relative to the starting mass on the system upon ignition of burners, with the resulting total mass lost with time for both experiments shown in Figure 6.

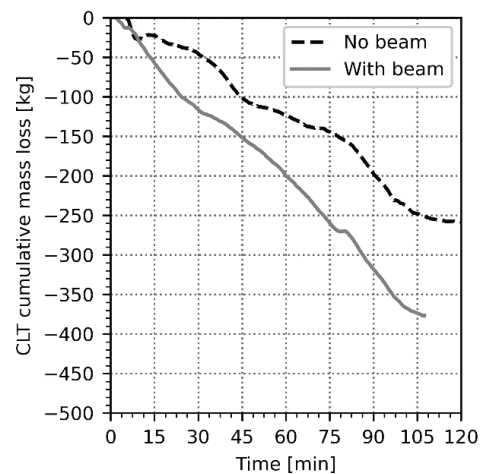


**Figure 6:** Comparison of total slab mass lost with time.

At the onset of the experiment, there was a c. 200 kg difference between the starting mass on the system for the “no beam” vs “with beam” case, which is largely attributable to the glulam beam mass, estimated at c. 40 kg/m.

Differentiating the mass lost with time and applying exponentially weighted smoothing over a 60 s period, gives the MLR, which has been presented per unit area in Figure 7. The MLR has been utilised alongside a net heat

of combustion of the timber of 17.5 +/- 2.5 MJ/kg to estimate the total heat release rate of the enclosure, when summed with the burner contribution given in Figure 2. The results are shown in Figure 8.

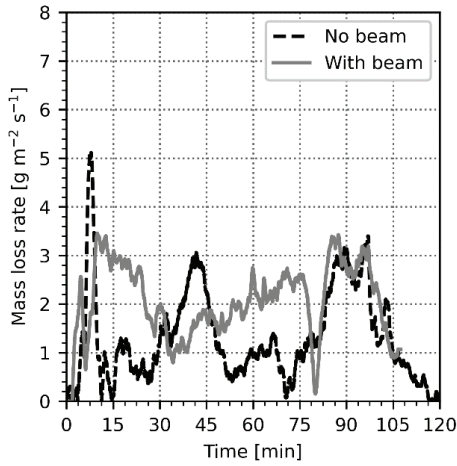


Figure 7: Comparison of slab mass loss rate with time.

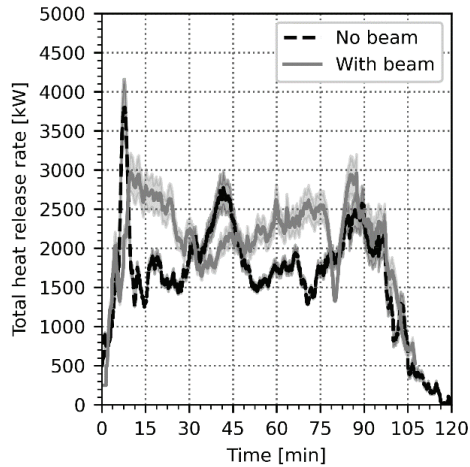


Figure 8: Comparison of total heat release rate with time, based on mean heat of combustion of 17.5 +/- 2.5 MJ/kg (shaded region)

### 3.2 Heat flux to the floor and ceiling

Ceiling and floor mounted plate thermometers (PT) were utilised to estimate the radiative heat flux to the surfaces, adopting the correlations presented in Wickstrom et al. [4], as adopted by other researchers for similar applications, e.g., Su et al. [5]. Neglecting the heat storage term of the energy balance of the PT, as per Ingason and Wickstrom [6], the radiative heat flux was derived according to Equation (1) and Table 1.

$$\dot{q}_{\text{inc}}'' = \frac{\epsilon_{\text{pt}} \sigma T_{\text{pt}}^4 + (h + K_{\text{cond}})(T_{\text{pt}} - T_{\infty})}{\epsilon_{\text{pt}}} \quad (1)$$

Resulting profiles of radiative heat flux relative to distance from the burner are shown in Figure 9 and Figure 10.

Table 1: Terms and constants adopted to estimate radiative heat flux to ceiling and floor, adopted from [7]

Parameter	Description	Value	Unit
$\epsilon_{\text{pt}}$	Emissivity of the PT	0.9	-
$\sigma$	Boltzmann constant	$5.67 \times 10^{-8}$	$\text{W} \cdot \text{m}^{-2} \cdot \text{K}^{-4}$
$h$	PT convection coefficient	10	$\text{W}/\text{m}^2 \cdot \text{K}$
$K_{\text{cond}}$	Conduction correction factor	8	$\text{W}/\text{m}^2 \cdot \text{K}$
$T_{\text{pt}}$	PT temperature	Varies	K
$T_{\infty}$	Ambient temperature	293	K

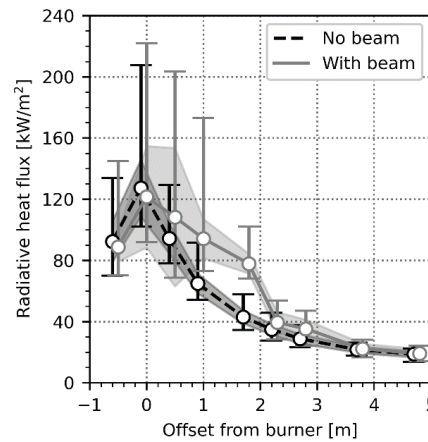


Figure 9: Radiative heat flux to the ceiling at different burner offsets, comparison of no beam vs. with beam. Burner HRR = 1,250 kW. Shaded envelope shows +/- one standard deviation, error bars show range of values.

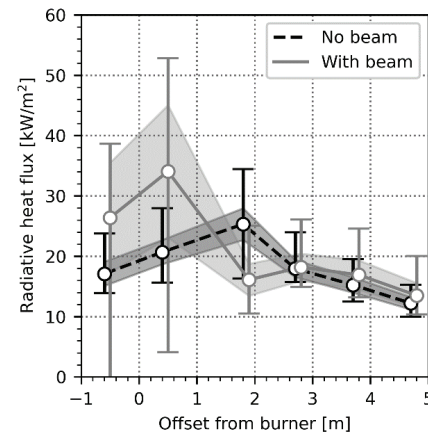
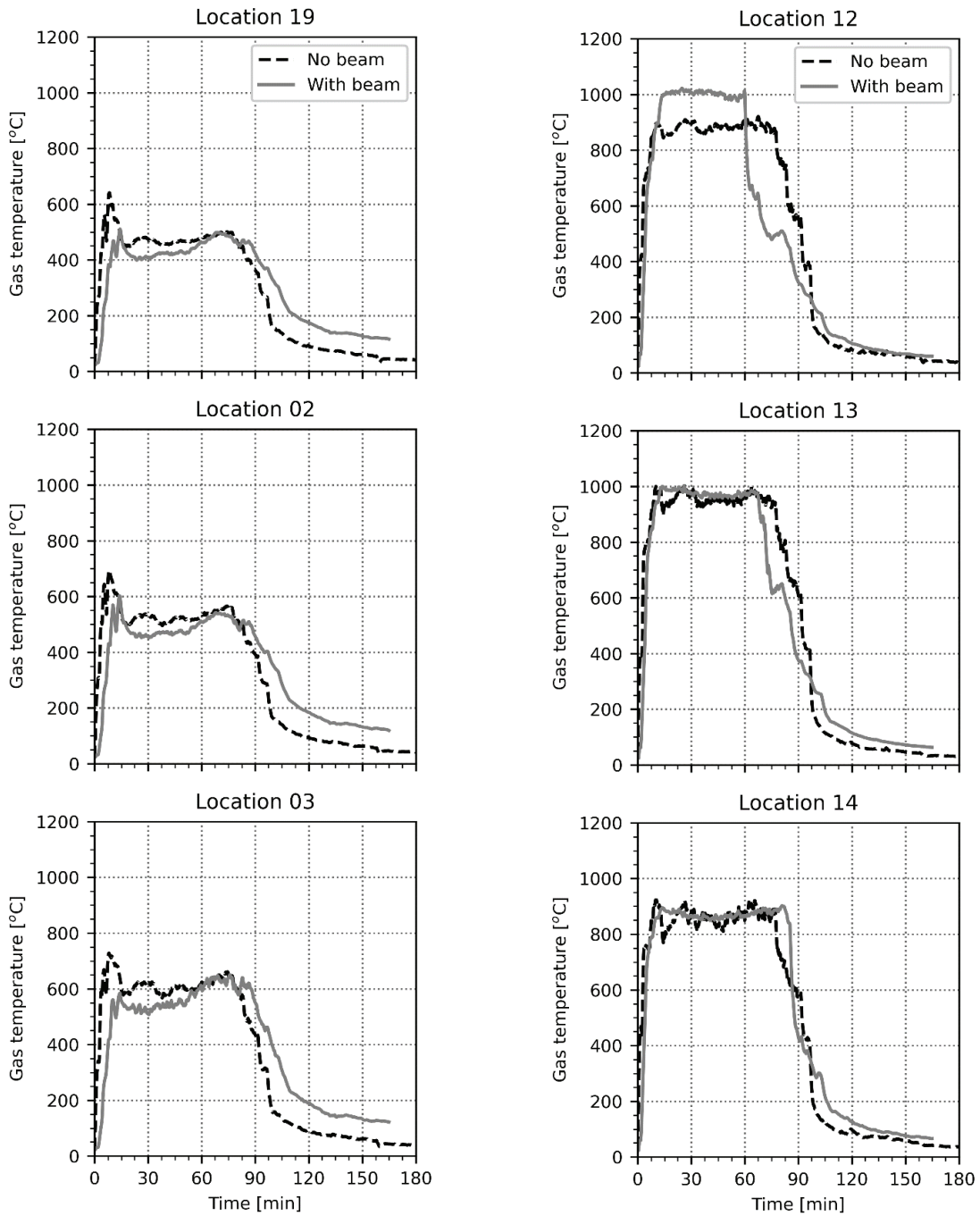


Figure 10: Radiative heat flux to the floor at different burner offsets, comparison of no beam vs. with beam. Burner HRR = 1,250 kW. Shaded envelope shows +/- one standard deviation, error bars show range of values.

### 3.3 Gas temperatures

Figure 11 and Figure 12 show the gas temperatures at ceiling level for the locations given in Figure 4.



**Figure 11:** Ceiling gas temperatures with time for locations 19, 02 and 03 (far field)

**Figure 12:** Ceiling gas temperatures with time for locations 12, 13 and 14 (near field)

## 4 DISCUSSION

### 4.1 Thermal exposure to the CLT soffit

Exposure to the CLT soffit can be distinguished by two zones, the near field and far field. The near field can broadly be taken as the ceiling area where burners impinged or resulted in a ceiling jet. This near field comprised slabs 1 and 2, with the far field slabs 3 and 4. In the case where a beam was included, this separated the near and far field.

In terms of the gas temperatures, Figure 11 showing results for the far field indicate no significant difference regardless of the inclusion of the glulam beam. Figure 12 for the near field shows increased gas temperatures in proximity to the glulam beam. This is likely a combination of (a) the flaming of the beam; and (b) a smoke reservoir effect, containing hot gases beneath slabs 1 and 2.

The increased gas temperatures correspond to increased heat fluxes to the ceiling in the near field, as evident in Figure 9 for the steady phase, where the burner HRR is 1250 kW. On the near field side of the beam, i.e., c. 1.8 m offset from the burner, the radiative heat flux ( $80 \text{ kW/m}^2$ ) is circa twice that observed for the flat ceiling case ( $40 \text{ kW/m}^2$ ).

Approximating the flame tip to coincide with a heat flux of c.  $20 \text{ kW/m}^2$  indicates that the beam did not reduce the flame extension at ceiling level. During the steady phase where the burner HRR is 1250 kW, flames extended over the full length of the ceiling in both cases.

### 4.2 Thermal exposure to the floor

In the near field, the beam increased the heat flux to the floor. At locations either side of the burner, the heat flux at the floor for the case with a beam was c. 150% of that without a beam, during the steady phase (burner HRR of 1250 kW).

The format of the experiments undertaken, i.e., with a discrete heat source and otherwise fuel load free enclosure, did not permit any direct evaluation of what the combustible ceiling might mean for flame spread rates within a large enclosure. However, the radiative heat flux to the floor provides insight as to what might be expected through benchmarking against complementary studies, such as that by Gupta et al. [8]. In their studies on mechanisms of flame spread in large enclosures, Gupta et al. observe a correlation between the external heat flux to the fuel in advance of the flame front and the flame front velocity. In a proposed phenomenological model, Gupta et al. postulated that as the external heat flux to the fuel in advance of the flame front converges on a critical ignition criterion (taken as  $10.5 \text{ kW/m}^2$  therein), the ratio of flame front to burn-out front velocity tends towards infinity, i.e., the flame spread rate is so fast so as to induce a “Mode 1” fire, which implies a fully developed post-flashover fire.

With reference to Figure 10, much of the floor in the far field receives a radiant heat flux significantly above  $10.5 \text{ kW/m}^2$ , implying that the combustion of the ceiling in either case would induce a change from a Mode 2 (growing fire) or Mode 3 fire (travelling fire) to Mode 1 (i.e., extremely rapid flame spread and transition to flashover). Such a rate of flame spread is supported by recent observations by Kotsovinos et al. [9] in their fire experiment in a  $352 \text{ m}^2$  enclosure with exposed CLT ceiling. In Kotsovinos et al.’s “CodeRed #01” experiment, once ignition of the ceiling occurred, flame spread over the cribs covering the full length of the enclosure was observed in under 3 min. The beam had little utility in reducing the heat flux to the floor in the far field, with similar values observed to the case without a beam. It may even be the case that the presence of a protrusion, such as a beam, could lead to more rapid fire spread as heat flux to the floor in vicinity of the flame front (burner in this case) was substantially higher.

### 4.3 Implications for mass loss and HRR

Revisiting Figure 6, the overall mass lost was greater for the case with the beam versus without. This, in part, is likely a result of an overall greater system mass, including both more combustible material and combustible surface area arising from the glulam beam.

The involvement of the combustible ceiling in both cases can be considered by contrasting the HRR of the burner in isolation (Figure 2) and the estimated total HRR, adopting load-cell data for the engineered timber ceiling (Figure 8). Upon ignition of the timber ceiling, the total HRR is around three times that of the burner in isolation, regardless of the inclusion of a beam. Post-ignition, the HRR for the case with a beam remains higher than without. This corresponds with the observation of generally higher ceiling heat fluxes in the near field attributed to the constraining of the ceiling jet and a marginally deeper smoke layer.

During the steady phase of the burner assault, i.e., from 8 to 88 min, MLR and, correspondingly, HRR, were higher for the case with a beam versus without. With the beam, the HRR was c. twice that of the burner in isolation. Without the beam, the HRR was c. one and a half that of the burner in isolation.

In both experiments, the flaming of the CLT was observed to stop over most of the exposed surface. Owing to the method of fixing of the glulam, i.e., stirrups versus screwing from above, flaming continued in the vicinity of the glulam beam requiring intervention to finally extinguish the combustion. This is reflected in the residual in MLR and HRR towards the end of the experiment, see Figure 7 and Figure 8.

### 4.4 Bond-line failure

Bond-line failure (BLF) leading to premature char fall-off was observed in both the experiment with and without the

glulam beam. For the case without the beam, this is shown in Figure 13. With the beam, the detached charred lamella is seen on the floor and on top of the burner in Figure 14.



**Figure 13:** Bond-line failure leading to premature char fall-off in experiment without beam.



**Figure 14:** Bond-line failure leading to premature char fall-off in experiment with beam. Detached char is apparent on floor and burner.

Despite the BLF and resulting premature char fall-off, flaming of the CLT ceiling was observed to stop. Due to the limited exposed combustible surface area, i.e., only a ceiling, upon turning off the burners, the heat flux to the engineered timber ceiling quickly dropped below thresholds typically associated with auto-extinction, see Figure 15. This suggests that for hybridised construction formats, where little interaction between combustible surfaces exists and combustible surfaces are generally limited to ceilings, averting BLF through more heat resistant adhesives is not a prerequisite for adequate structural performance in the event of fire. However, it does require the designer to consider BLF in terms of the impact on structural capacity.

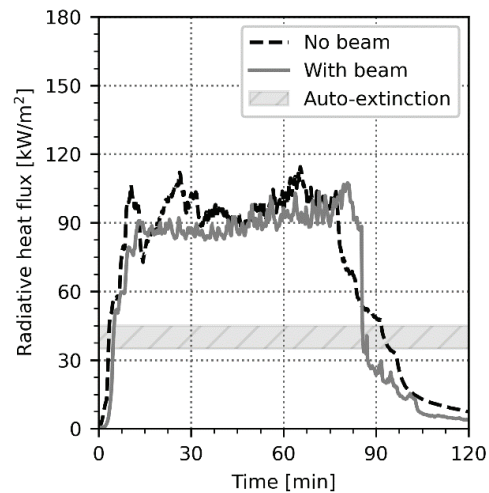


**Figure 15:** Radiative heat flux with time to the ceiling at location 14.

## 5 CONCLUSIONS

Two experiments are reported herein that are part of a larger body of research work. This paper has focused on the differences between exposed engineered timber ceilings that either include a beam (a glulam beam with CLT slabs) or feature a flat soffit (only CLT). In both experiments, the only variable is the beam which results in a ceiling protrusion. All other parameters, i.e., the CLT type, lay-up and adhesive, burner HRR and instrumentation remained the same. Considering the impact of the down-stand beam, it can be concluded that:

- The presence of the beam locally increased heat fluxes to the ceiling in the near field relative to the case without a beam. In proximity to the beam, this increase was around a factor of two and is attributed to a combination of the constraining of the ceiling jet and a deeper smoke layer.
- The increased heat flux to the ceiling translated to an increase in heat flux to the floor when considered relative to the case without a beam.
- The beam had little impact on reducing the flame lengths at ceiling level, with flaming observed over the full extent of the ceiling in both experiments once the burner HRR reached 1250 kW.
- The increased heat fluxes in the case with a beam present resulted in both a higher overall mass lost by the engineered timber ceiling and total heat release rate.

In more general terms, it is noteworthy that regardless of the presence of a beam, auto-extinction of flaming combustion of the CLT was observed to occur in both experiments. This was despite bond-line failures in both experiments, leading to premature char fall-off. In the

case with a beam, flaming continued in proximity to the glulam beam, which was attributed to the method of fixing, with the beam held in place from below via stirrups. This allowed a gap to develop between the top of the CLT and glulam beam, where flaming persisted, ultimately requiring intervention.

Based upon the findings of other studies conducted as part of the larger STA project, it is expected that the results of these experiments would be applicable to CLT manufactured by different suppliers, subject to consistency in moisture content, adhesive type, edge-bonding condition, CLT thickness and CLT lay-up. Studies reported in Hopkin et al. [10] noted there to be nominal differences in the fire behaviour characteristics of CLT from three different leading suppliers, subject to the same specification parameters. It is expected that such a small-scale testing format/regime could be utilised to inform whether the data developed from the large-scale experiments reported herein could be applicable to a given product/supplier.

## ACKNOWLEDGEMENTS

The authors wish to acknowledge the contributions of the wider STA project team, including the discussions and technical contributions made by the Structural Timber Association (STA), BK Structures and Eurban.

## REFERENCES

- [1] Structural Timber Association, Structural timber buildings fire safety in use guidance. Volume 6 - Mass timber structures; Building Regulation compliance B3(1), V1.1. Structural Timber Association, 2020.
- [2] S. Nothard, D. Lange, J. P. Hidalgo, V. Gupta, and M. S. McLaggan, 'The response of exposed timber in open plan compartment fires and its impact on the fire dynamics', in Proceedings of the 11th International Conference on Structures in Fire (SiF2020), Online, Nov. 2020. doi: 10.14264/5d97785.
- [3] D. Hopkin et al., 'Large-scale enclosure fire experiments adopting CLT slabs with different types of polyurethane adhesives: Genesis and preliminary findings', *Fire*, vol. 5, no. 2, Art. no. 2, Apr. 2022, doi: 10.3390/fire5020039.
- [4] U. Wickström, J. Anderson, and J. Sjöström, 'Measuring incident heat flux and adiabatic surface temperature with plate thermometers in ambient and high temperatures', *Fire and Materials*, vol. 43, no. 1, pp. 51–56, Jan. 2019, doi: 10.1002/fam.2667.
- [5] J. Su, P.-S. Lafrance, M. Hoehler, and M. Bundy, 'Fire safety challenges of tall wood buildings – Phase 2: Task 2 & 3 – Cross laminated timber compartment fire tests', Fire Protection Research Foundation, Quincy, FPRF-2018-01, 2018.
- [6] H. Ingason and U. Wickström, 'Measuring incident radiant heat flux using the plate thermometer', *Fire Safety Journal*, vol. 42, no. 2, pp. 161–166, Mar. 2007, doi: 10.1016/j.firesaf.2006.08.008.
- [7] A. Häggkvist, J. Sjöström, and U. Wickström, 'Using plate thermometer measurements to calculate incident heat radiation', *Journal of Fire Sciences*, vol. 31, no. 2, pp. 166–177, Mar. 2013, doi: 10.1177/0734904112459264.
- [8] V. Gupta, A. F. Osorio, J. L. Torero, and J. P. Hidalgo, 'Mechanisms of flame spread and burnout in large enclosure fires', Proceedings of the Combustion Institute, vol. 38, no. 3, pp. 4525–4533, 2021, doi: 10.1016/j.proci.2020.07.074.
- [9] P. Kotsovinos et al., 'Fire dynamics inside a large and open-plan compartment with exposed timber ceiling and columns: CODERED #01 ', *Fire and Materials*, p. fam.3049, Feb. 2022, doi: 10.1002/fam.3049.
- [10] D. Hopkin et al., 'Experimental characterisation of the fire behaviour of CLT ceiling elements from different leading suppliers', in Applications of Structural Fire Engineering, Ljubljana, Slovenia, 2021.